

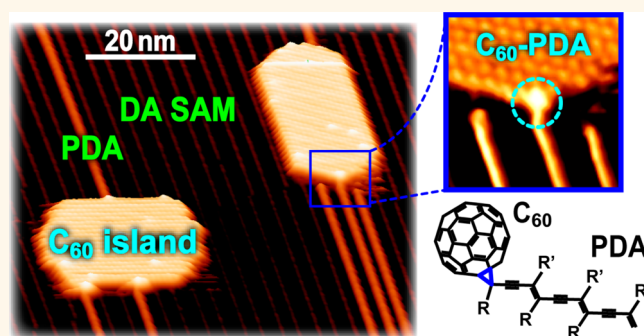
Nanojunction between Fullerene and One-Dimensional Conductive Polymer on Solid Surfaces

Masato Nakaya,[†] Yuji Okawa,[†] Christian Joachim,^{†,‡} Masakazu Aono,[†] and Tomonobu Nakayama^{*,†,§}

[†]International Center for Materials Nanoarchitectonics (WPI-MANA), National Institute for Materials Science (NIMS), 1-1 Namiki, Tsukuba, Ibaraki 305-0044, Japan,

[‡]Centre d'Elaboration de Matériaux et d'Études Structurales (CEMES), Centre National de la Recherche Scientifique (CNRS), 29 rue J. Marvig, 31055 Toulouse Cedex, France, and [§]Graduate School of Pure and Applied Sciences, University of Tsukuba, 1-1 Namiki, Tsukuba, Ibaraki 305-0044, Japan

ABSTRACT Bottom-up creation of huge molecular complexes by covalently interconnecting functional molecules and conductive polymers is a key technology for constructing nanoscale electronic circuits. In this study, we have created an array of molecule–polymer nanojunctions from C₆₀ molecules and polydiacetylene (PDA) nanowires at designated positions on solid surfaces by controlling self-assemblies and intermolecular chemical reactions of molecular ingredients predeposited onto the surfaces. In the proposed method, the construction of each nanojunction spontaneously proceeds *via* two types of chemical reactions: a chain polymerization among self-assembled diacetylene compound molecules for creating a single PDA nanowire and a subsequent cycloaddition reaction between the propagating forefront part of the PDA backbone and a single C₆₀ molecule adsorbed on the surface. Scanning tunneling microscopy has proved that the C₆₀ molecule is covalently connected to each end of the π -conjugated PDA backbone. Furthermore, the decrease in the energy gap of the C₆₀ molecule in nanojunctions is observed as compared with that of pristine C₆₀ molecules, which is considered to be due to the covalent interaction between the PDA edge and the C₆₀ molecule.



KEYWORDS: fullerene · polymer · STM · molecular electronics · heterojunction

Construction of electronics using only molecular-based components is one of the ultimate goals in recent molecular science and technology fields.^{1–4} Since individual organic molecules behave as unit elements exhibiting peculiar physicochemical properties, the creation of nanoscale heterojunctions by interconnecting two types of molecules in combinations of donor–acceptor, host–guest, and so forth offers molecular-scale active elements of nanodevices exhibiting sophisticated functions such as electrical rectification,⁵ switching,^{6–8} photoelectric conversion,⁹ and logical operation.¹⁰ In particular, creating an array of the nanojunctions between the one-dimensional (1D) conductive polymers and functional molecules has practical advantages for realizing the molecular circuitry¹¹ because the 1D polymer is expected to behave not only as a part of nanojunction but also as an electric wire.^{12,13} An essential

requirement in this concept is to connect the functional molecules to the 1D polymer *via* covalent bonds, which realizes well-defined physical and/or electrical contact in the nanojunction and improves its performance such as structural stability and/or efficiency of charged-carrier transfers. Although such a molecule–polymer system would be finely created by advanced chemical synthesis in the liquid phase, it is difficult to arrange such huge molecular assemblies on solid surfaces while remaining intact. In contrast, it has recently been demonstrated that some macromolecules such as polymers and huge molecular complexes can be synthesized on solid surfaces by controlling covalent assembly among molecular building blocks deposited onto the surfaces.^{12,14–18} This methodology also allows us to investigate pristine geometry and electronic properties with atomic resolution of such macromolecular systems by scanning tunneling

* Address correspondence
nakayama.tomonobu@nims.go.jp.

Received for review August 1, 2014
and accepted December 3, 2014.

Published online December 03, 2014
10.1021/nn504275b

© 2014 American Chemical Society

microscopy and spectroscopy (STM/STS). In this study, we have fabricated an array of molecule-polymer nanojunctions on solid surfaces using C_{60} molecules¹⁹ and 1D polymer nanowires of diacetylene (DA) compound molecules, polydiacetylenes (PDAs),¹² in which the C_{60} molecule is covalently bound to an end of a π -conjugated PDA moiety.

The C_{60} -PDA nanojunctions have been fabricated by the chemical soldering method.^{12,20} The key to this method is the linear chain polymerization in the self-assembled monolayer (SAM) of DA molecules, as shown in Figures 1B,C, which is induced *via* electronic excitation of DA molecules by electrons inelastically tunneling between an STM tip and substrates or by photons irradiated from an ultraviolet (UV) light source. In the chain polymerization, a DA moiety in a single monomer molecule is first excited as a reactive diradical. Then a dimer is created by an addition reaction between the radical and a neighboring DA molecule. Since the created dimer also has reactive terminals, the 1D polymer is extended by spontaneously repeating the addition reactions along a molecular row of DA moieties in the SAM.^{12,20} Interestingly, the propagating reactive terminal of the PDA reacts not only with a neighboring DA molecule but also with different molecular species adsorbed on the row of DA moieties.^{12,20} However, despite the simplicity, versatility, and potential ability of this method to create an array of polymer-molecule nanojunctions on solid surfaces, it has been demonstrated only for fabricating a nanojunction between a PDA nanowire and a single phthalocyanine molecule. In the current study, we have shown that this method is also useful for covalently connecting the PDA nanowire to a C_{60} molecule *via* cycloaddition reaction.

RESULTS AND DISCUSSION

Figure 2A shows an STM image of a clean surface of MoS_2 obtained after simultaneously depositing 1.0 and 0.1 ML of DA compound and C_{60} molecules, respectively, at room temperature (rt). In this work, 10,12-pentacosadiynoic acid [$R-C\equiv C-C\equiv C-R'$, where $C\equiv C-C\equiv C$, R, and R' correspond to the DA moiety, $CH_3(CH_2)_{11}$, and $(CH_2)_8COOH$ side chains, respectively] was used as the DA compound molecule. The regions A and B in Figure 2A correspond to a SAM and monolayer islands of DA and C_{60} molecules, respectively, as discussed below. Similar structures have also been prepared on clean surfaces of highly oriented pyrolytic graphite (HOPG). In the high-resolution image of region A (Figure 2B), parallel bright lines separated by about ~ 3.0 and ~ 4.0 nm are observed. In addition, an array of slightly bright spots along the bright lines with a separation of ~ 0.5 nm is also observed in Figure 2B. According to the previous STM studies on SAMs of the same DA compound molecules formed by Langmuir-Schaefer (LS) and drop casting

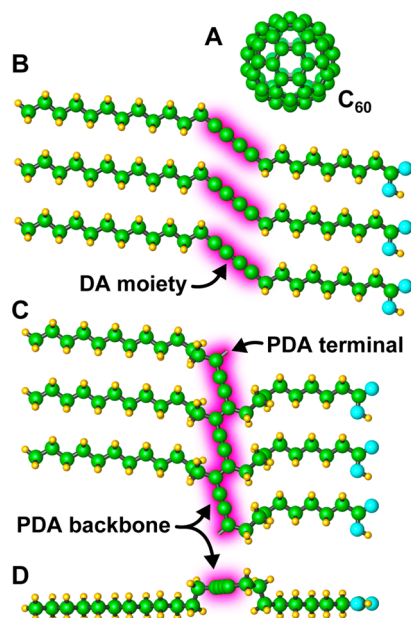


Figure 1. Molecular structures of (A) C_{60} , (B) monomers, and (C) a polymer of 10,12-pentacosadiynoic acid. (D) Side view of (C). Filled circles of green, blue, and yellow correspond to carbon, oxygen, and hydrogen atoms, respectively.

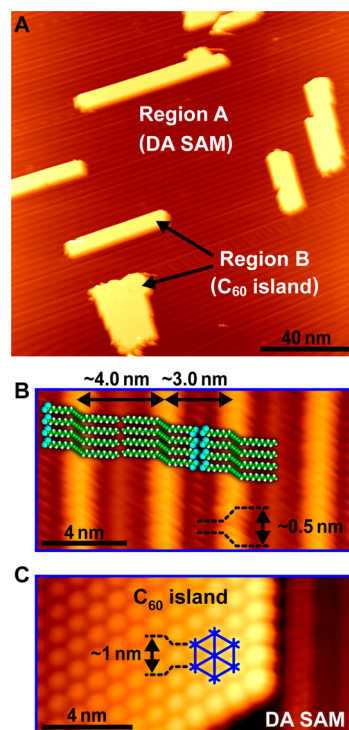


Figure 2. (A) Wide-scale STM image of C_{60} nanoislands and the DA SAM formed on the MoS_2 surface. (B, C) High-resolution STM images taken on the DA SAM and the C_{60} nanoisland, respectively, which are formed on HOPG surfaces. The inset in (B) is a model of molecular arrangement in the DA SAM. The imaging conditions (V_s and I_t) are 2 V and 25 pA for (A), -2.1 V and 30 pA for (B), and -2 V and 30 pA for (C).

methods,^{20–23} the DA SAM is composed of molecules lying flat on the substrate surface and aligning parallel to each other with an intermolecular distance of

0.47 nm, as shown in the inset of Figure 2B. In these films formed by LS and drop-casting methods, the aligned DA moieties are observed as bright lines with spacings of 3.0 and 3.8 nm in STM images because DA molecules are arranged in a manner such that the COOH end-groups of the chain are opposite to those of a neighboring molecule. The observed periodicity in region A agrees well with those of the DA films formed by LS and drop-casting methods.

Figure 2C shows a high-resolution STM image taken at the boundary between the DA SAM and a C_{60} island with a single-molecule height. The C_{60} island is composed of hexagonally ordered C_{60} molecules with an intermolecular distance of ~ 1.0 nm. This ordering is similar to that in the multilayer films consisting of closely packed C_{60} molecules.²⁴ The arrangement of C_{60} molecules is maintained during the lateral growth of the C_{60} islands by the additional deposition of C_{60} molecules until the monolayer C_{60} film covering over the DA SAM (see section 1 in Supporting Information), although there is a large lattice mismatch between the monolayer film of closely packed C_{60} molecules and the DA SAM. This result is different from the cases of C_{60} adlayer formation on SAMs of cyclothiophenes,²⁵ α -sexithiophenes,²⁶ acridine-9-carboxylic acids,²⁷ zinc porphyrin derivatives,²⁸ and so forth, on which the arrangement of C_{60} molecules is strongly modified by a donor–acceptor interaction between C_{60} molecules and the SAMs. It is also important to point out that, in our experiments, although the DA and C_{60} molecules were simultaneously deposited at various rates onto the MoS_2 and HOPG surfaces, molecular-scale mixtures²⁹ have never been created on surfaces. The above experimental observations indicate that the interaction between C_{60} and DA molecules are much smaller than the van der Waals ones interaction between C_{60} molecules. This is consistent with another fact that C_{60} molecules in the island are observed as smooth spheres (Figure 2C), indicating that each C_{60} molecule freely rotates on the DA SAM similar to those on chemically inert surfaces.³⁰

The C_{60} –DA interaction is locally modified by inducing chain polymerizations between the DA molecules. In the following example, chain polymerization was induced by irradiating UV light under ultrahigh vacuum (UHV) using a low-pressure mercury lamp (wavelength of ~ 254 nm and power density of ~ 1.3 mW/cm²) for 60 min. Figure 3A shows an STM image of a DA SAM and C_{60} islands after irradiating the UV light. An array of nanowires exhibiting very bright image contrast corresponds to PDA backbones created by the chain polymerization between DA molecules, as discussed in the previous STM studies.^{12,20–23} The bright image contrast of the PDA backbone simultaneously originates from its geometrical lift-up by 0.15 nm (Figure 1D) and a closure of its HOMO–LUMO gap near the Fermi level (E_F) as compared with the DA

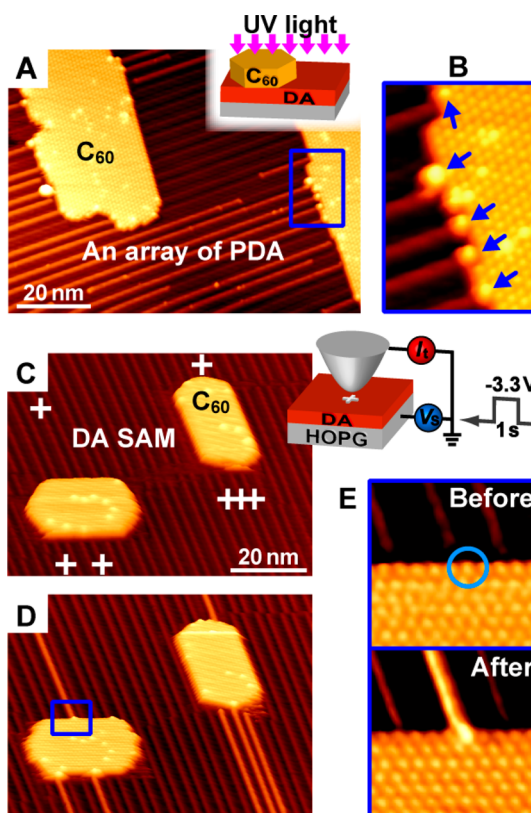


Figure 3. Creation of nanojunctions between C_{60} nanoislands and PDA nanowires. (A) Wide-scale STM image taken after inducing the chain polymerization by irradiating UV light for the overall region on the surface. (B) Magnified image of the region surrounded by a blue line in (A). (C) and (D) STM images taken before and after inducing chain polymerization by applying V_s of -3.3 V at the positions indicated by crosses in (C) for 1 s, respectively. (E) Magnified image of the region surrounded by a blue line in (D). DA SAMs and C_{60} islands were formed on HOPG surfaces. The imaging conditions (V_s and I_t) are -2.2 V and 20 pA for (A) and (B) and -2 V and 30 pA for (C)–(E).

monomers.^{12,20,31} Figure 3B shows the magnified image of the region surrounded by the blue line in Figure 3A, in which C_{60} molecules in contact with each end of PDA nanowires (blue arrows) exhibit a bright image contrast. The correlation between the change in the image contrast of the C_{60} molecule and the formation of the PDA nanowire is clearly demonstrated by the following experiments. Parts C and D of Figure 3 show STM images of two C_{60} islands formed on a DA SAM, which were taken before and after the STM-induced chain polymerization, respectively, triggered by applying sample bias voltage (V_s) of -3.3 V for 1 s at each tip position indicated by crosses in Figure 3C. After these procedures, seven PDA nanowires were created along an array of DA moieties and terminated by edges of C_{60} nanoislands, as shown in Figure 3D. Upper and lower panels in Figure 3E show magnified images of the region surrounded by the blue line in Figure 3D taken before and after creating a single PDA nanowire, respectively. Comparing them, it is clearly observed that the single C_{60} molecule exhibits

a brighter image contrast after connecting with the PDA nanowire. This bright appearance is considered to originate mainly from the energy shift of the frontier molecular orbitals of the C_{60} molecule, which is considered to occur by covalent bonding to the end of the PDA nanowire, as discussed latter. The C_{60} molecule behaves as an anchor part for the physical and electronic contacts between the C_{60} island and a PDA nanowire.

We have gained experimental evidence that the C_{60} molecule is strongly bound to the end of the PDA nanowire. In this study, C_{60} molecules deposited onto DA SAMs were not observed as isolated single-molecule adsorbates but mostly as islands and sometimes as a two-dimensional (2D) gas phase of C_{60} molecules. The 2D gas phase was recognized as a noisy feature around C_{60} islands in STM images. Figure 4A shows an STM image of the 2D gas-phase C_{60} molecules around a C_{60} island, which was observed after inducing chain polymerization by UV light irradiation. Interestingly, we recognize that four single C_{60} molecules are immobilized with each end of four PDA nanowires in the vicinity of the 2D gas as indicated by blue dotted circles. Furthermore, the C_{60} molecule immobilized with the PDA nanowire sometimes exhibits internal structures at RT as shown in the inset of Figure 4A, clearly indicating that the rotational motion of the C_{60} molecule is inhibited. Such an inhibition of molecular rotation has been reported for the C_{60} molecules cross-linked via [2 + 2] cycloadditive four-membered rings.^{30,32} These results strongly suggest that the C_{60} molecules diffusing on the surface have accidentally encountered and reacted with a propagating forefront part of PDA in which reactive chemical species (carbene or radical) appear.³³ In addition, we have obtained further evidence that each C_{60} molecule is strongly connected to the end of a PDA nanowire. When PDA nanowires are connected to C_{60} molecules located at the edge of a C_{60} island (e.g., Figure 3A,D), the lateral position of each anchor C_{60} molecule is often shifted from its original position in the C_{60} island (see section 2 in the Supporting Information), suggesting that the anchor C_{60} molecule is strongly bound to the PDA nanowire and finally relaxed at the observed position.

Figure 4B shows a possible chemical reaction between the PDA and the C_{60} molecule, where the carbene at the forefront part of PDA reacts to the 6–6 part in the C_{60} molecule, resulting in the double bond of the C_{60} molecule being cleaved and the formation of three-membered ring via [1 + 2] cycloaddition reaction as an intermolecular bond. Although similar chemical reactions between various carbene species and C_{60} molecules have been widely used in the chemical synthesis of C_{60} derivatives,^{34–37} the present result is the first demonstration of this type of chemical reaction in the surface synthesis of huge molecular complexes.

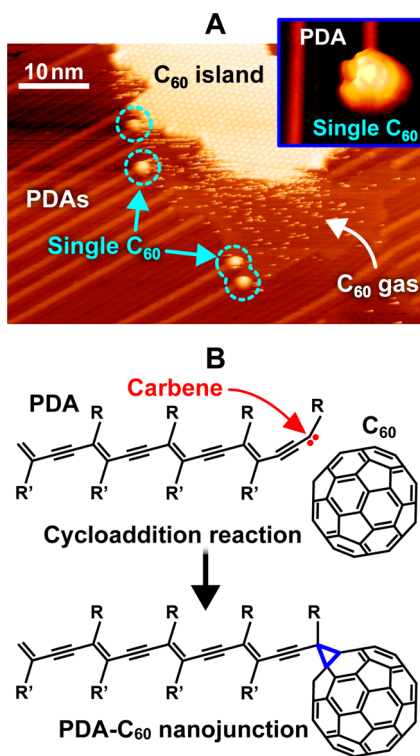


Figure 4. Covalent bonding between a single C_{60} molecule and an end of PDA nanowire. (A) STM image of the nanoisland and 2D gas of C_{60} molecules on the DA SAM, taken after inducing chain polymerization between DA molecules. The sample was formed on a HOPG surface. The inset in (A) shows a high-resolution image of a single C_{60} molecule connecting to a PDA nanowire. The imaging conditions of (A) and its inset are V_s of -2.3 V and I_t of 20 pA. (B) Cycloaddition reaction between C_{60} molecules and PDA nanowire, which is possible candidate for the chemical reaction creating C_{60} -PDA nanojunctions.

It has also been found that the frontier molecular orbitals of C_{60} molecule are shifted in energy after reacting with the end of a PDA nanowire. Figure 5 shows the tip-height profiles determined by STM along the lines intersecting an anchor C_{60} molecule in a C_{60} island connected to PDA and other molecules existing in the island, for example as shown by a dotted line in the inset. Blue and red curves are taken by STM scans at filled ($V_s < 0$) and empty ($V_s > 0$) states of each C_{60} -PDA junction formed on HOPG and MoS_2 surfaces, respectively. Some profiles show that the tip height is higher on the anchor C_{60} molecule than on the other C_{60} molecules in the islands. This corresponds to the above result that the anchor C_{60} molecule exhibits a brighter appearance than the other molecules in STM images. Interestingly, the tip-height profiles over the anchor C_{60} molecule change depending on the bias voltage in both bias polarities, strongly indicating that the electronic structure of the anchor C_{60} molecule is modified. Although the highest occupied molecular orbital (HOMO) and lowest unoccupied molecular orbital (LUMO) levels of pristine C_{60} molecules adsorbed on the surface of a DA SAM appear at $V_s < -2.5$ V and $V_s \approx +1.4$ V, respectively, in the

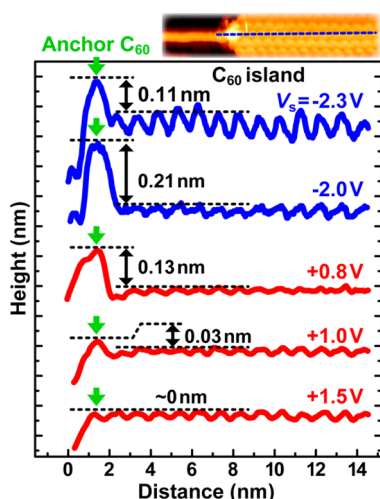


Figure 5. Cross-sectional profiles along lines intersecting C_{60} molecule closely connecting to a PDA (each green arrow) and the others existing in C_{60} nanoisland, which are taken at V_s of -2.3 , -2.0 , 0.8 , 1.0 , and 1.5 V. Blue and red curves were taken along C_{60} –PDA junctions formed on HOPG and MoS_2 surfaces, respectively.

STS measurement (see section 3 in the Supporting Information), the tip-height difference becomes considerable at a smaller bias. This fact implies that the HOMO–LUMO gap of the anchor C_{60} molecule is smaller than that of the pristine C_{60} molecule. This consideration is qualitatively consistent with the preceding conclusion that the C_{60} molecule is covalently bound to the PDA nanowire, because it is known that the energy gap of a C_{60} molecule decreases by covalent bonding with surfaces^{38,39} or other molecular species,⁴⁰ which originates from the degeneration of HOMO and/or LUMO levels owing to the impairment of the symmetrical molecular structure.

On the other hand, since the DA SAM behaves as a thin insulating layer between C_{60} molecules and the conductive substrate, connecting the C_{60} molecule to a conductive polymer would increase the electronic coupling between the C_{60} molecule and the substrate, which is another possible cause for the

bright appearance of the C_{60} molecule in the STM imaging of C_{60} –PDA junctions, similar to the case of lander molecules connecting at the step edge of the metallic substrate.^{41,42} Toward a better understanding of the present results, further clarification regarding the geometry and energy level alignment of the C_{60} –PDA nanojunction should be carried out. STS measurements at lower temperatures after creating C_{60} –PDA nanojunctions at RT would be ideal for the detail clarification. In addition, theoretical calculations could provide us insights into the electrical properties of the C_{60} –PDA nanojunction such as the low voltage electronic conductance, the current–voltage characteristics, and the effective injection barrier of charged-carriers of this molecule–polymer nanojunction.

CONCLUSIONS AND PROSPECTS

To summarize, the nanoscale heterojunction composed of the C_{60} molecule and the PDA nanowire has been constructed on solid surfaces. In this nanojunction, a single C_{60} molecule is covalently bound to the end of a π -conjugated PDA backbone. The covalent interaction between them is considered to reduce the HOMO–LUMO gap of the C_{60} molecule in the C_{60} –PDA nanojunction. This C_{60} –PDA nanojunction considers the huge molecular complex created only by our chemical soldering experiments on solid surfaces. Further clarification of the geometry and electronic structures of the C_{60} –PDA molecular junction can reveal its functionalities and properties, *e.g.*, conduction and injection properties of electrons, holes, and polarons between two closely connected π -conjugated parts. Another challenge is to actively control the formation and annihilation of the covalent bond between the C_{60} molecule and the PDA nanowire, such as that realized between C_{60} molecules.^{30,32,43} The current results and further challenges would lead to the realization of molecular nanoelectronics using molecule–polymer nanojunctions.

EXPERIMENTAL METHODS

Sample Preparation. All experiments were carried out in an UHV chamber with a base pressure of 1.0×10^{-8} Pa. The DA SAM and C_{60} nanoislands were formed by simultaneously depositing DA compound and C_{60} molecules at rt onto clean surfaces of HOPG and MoS_2 . The HOPG and MoS_2 were cleaved in air followed by thermal annealing at 500 °C in UHV. Depositions of DA and C_{60} molecules were carried out by the thermal evaporation of molecular powders with purities of above 97% and 99.995% from a Ta boat and BN crucible while maintaining deposition rates of 0.1 and 0.01 ML/min, respectively. All the STM experiments were carried out using an electrochemically etched Pt–20%Ir tip at rt in UHV.

Conflict of Interest: The authors declare no competing financial interest.

Supporting Information Available: STM observation of a DA SAM after covering with a C_{60} monolayer film, positional change of C_{60} molecules with formation of C_{60} –PDA nanojunctions, and STS measurements of C_{60} molecules and PDA nanowires.

This material is available free of charge via the Internet at <http://pubs.acs.org>

REFERENCES AND NOTES

- Joachim, C.; Gimzewski, J. K.; Aviram, A. Electronics Using Hybrid-Molecular and Mono-Molecular Devices. *Nature* **2000**, *408*, 541–548.
- Donhauser, Z. J.; Mantoosh, B. A.; Kelly, K. F.; Bumm, L. A.; Monnell, J. D.; Stapleton, J. J.; Price, D. W., Jr.; Rawlett, A. M.; Allara, D. L.; Tour, J. M.; *et al.* Conductance Switching in Single Molecules through Conformational Changes. *Science* **2001**, *292*, 2303–2307.
- Tao, N. J. Electron Transport in Molecular Junctions. *Nat. Nanotechnol.* **2006**, *1*, 173–181.
- Song, H.; Reed, M. A.; Lee, T. Single Molecule Electronic Devices. *Adv. Mater.* **2011**, *23*, 1583–1608.
- Aviram, A.; Ratner, M. A. Molecular Rectifiers. *Chem. Phys. Lett.* **1974**, *29*, 277–283.

6. Gao, H. J.; Sohlberg, K.; Xue, Z. Q.; Chen, H. Y.; Hou, S. M.; Ma, L. P.; Fang, X. W.; Pang, S. J.; Pennycook, S. J. Reversible, Nanometer-Scale Conductance Transitions in an Organic Complex. *Phys. Rev. Lett.* **2000**, *84*, 1780–1783.
7. Pathem, B. K.; Claridge, S. A.; Zheng, Y. B.; Weiss, P. S. Molecular Switches and Motors on Surfaces. *Annu. Rev. Phys. Chem.* **2013**, *64*, 605–630.
8. Yang, Y.-W.; Sun, Y.-L.; Song, N. Switchable Host-Guest Systems on Surfaces. *Acc. Chem. Res.* **2014**, *47*, 1950–1960.
9. Imahori, H.; Tamaki, K.; Guldi, D. M.; Luo, C.; Fujitsuka, M.; Ito, O.; Sakata, Y.; Fukuzumi, S. Modulating Charge Separation and Charge Recombination Dynamics in Porphyrin-Fullerene Linked Dyads and Triads: Marcus-Normal versus Inverted Region. *J. Am. Chem. Soc.* **2001**, *123*, 2607–2617.
10. Witlicki, E. H.; Johnsen, C.; Hansen, S. W.; Silverstein, D. W.; Bottomley, V. J.; Jeppesen, J. O.; Wong, E. W.; Jensen, L.; Flood, A. H. Molecular Logic Gates using Surface-Enhanced Raman-Scattered Light. *J. Am. Chem. Soc.* **2011**, *133*, 7288–7291.
11. Wada, Y.; Tsukada, M.; Fujihira, M.; Matsushige, K.; Ogawa, T.; Haga, M.; Tanaka, S. Prospects and Problems of Single Molecule Information Devices. *Jpn. J. Appl. Phys.* **2000**, *39*, 3835–3849.
12. Okawa, Y.; Mandal, S. K.; Hu, C.; Tateyama, Y.; Goedecker, S.; Tsukamoto, S.; Hasegawa, T.; Gimzewski, J. K.; Aono, M. Chemical Wiring and Soldering toward All-Molecule Electronic Circuitry. *J. Am. Chem. Soc.* **2011**, *133*, 8227–8233.
13. Umeyama, T.; Tezuka, N.; Kawashima, F.; Seki, S.; Matano, Y.; Nakao, Y.; Shishido, T.; Nishi, M.; Hirao, K.; Lehtivuori, H.; *et al.* H. Carbon Nanotube Wiring of Donor-Acceptor Nanograins by Self-Assembly and Efficient Charge Transport. *Angew. Chem.* **2011**, *123*, 4711–4715.
14. Hla, S.-W.; Bartels, L.; Meyer, G.; Rieder, K.-H. Inducing All Steps of a Chemical Reaction with the Scanning Tunneling Microscope Tip: Towards Single Molecule Engineering. *Phys. Rev. Lett.* **2000**, *85*, 2777–2780.
15. Sakaguchi, H.; Matsumura, H.; Gong, H.; Abouelwafa, A. M. Direct Visualization of the Formation of Single-Molecule Conjugated Copolymers. *Science* **2005**, *310*, 1002–1006.
16. Treier, M.; Richardson, N. V.; Fasel, R. Fabrication of Surface-Supported Low-Dimensional Polyimide Networks. *J. Am. Chem. Soc.* **2008**, *130*, 14054–14055.
17. Cai, J.; Ruffieux, P.; Jaafar, R.; Bieri, M.; Braun, T.; Blankenburg, S.; Muoth, M.; Seitsonen, A. P.; Saleh, M.; Feng, X.; *et al.* R. Atomically Precise Bottom-Up Fabrication of Graphene Nanoribbons. *Nature* **2010**, *466*, 470–473.
18. Lafferentz, L.; Eberhardt, V.; Dri, C.; Africh, C.; Comelli, G.; Esch, F.; Hecht, S.; Grill, L. Controlling On-Surface Polymerization by Hierarchical and Substrate-Directed Growth. *Nat. Chem.* **2012**, *4*, 215–220.
19. Kroto, H. W.; Heath, J. R.; O'Brien, S. C.; Curl, R. F.; Smalley, R. E. C₆₀: Buckminsterfullerene. *Nature* **1985**, *318*, 162–163.
20. Okawa, Y.; Akai-Kasaya, M.; Kuwahara, Y.; Mandal, S. K.; Aono, M. Controlled Chain Polymerisation and Chemical Soldering for Single-Molecule Electronics. *Nanoscale* **2012**, *4*, 3013–3028.
21. Giridharagopal, R.; Kelly, K. F. Substrate-Dependent Properties of Polydiacetylene Nanowires on Graphite and MoS₂. *ACS Nano* **2008**, *2*, 1571–1580.
22. Okawa, Y.; Aono, M. Linear Chain Polymerization Initiated by a Scanning Tunneling Microscope Tip at Designated Positions. *J. Chem. Phys.* **2001**, *115*, 2317–2322.
23. Mandal, S. K.; Okawa, Y.; Hasegawa, T.; Aono, M. Rate-Determining Factors in the Chain Polymerization of Molecules Initiated by Local Single-Molecule Excitation. *ACS Nano* **2011**, *5*, 2779–2786.
24. Núñez-Regueiro, M.; Marques, L.; Hodeau, J.-L.; Béthoux, O.; Perroux, M. Polymerized Fullerite Structures. *Phys. Rev. Lett.* **1995**, *74*, 278–281.
25. Mena-Osteritz, E.; Bäuerle, P. Complexation of C₆₀ on a Cyclophane Monolayer Template. *Adv. Mater.* **2006**, *18*, 447–451.
26. Chen, L.; Chen, W.; Huang, H.; Zhang, H. L.; Yuhara, J.; Wee, A. T. S. Tunable Arrays of C₆₀ Molecular Chains. *Adv. Mater.* **2008**, *20*, 484–488.
27. Xu, B.; Tao, C.; Williams, E. D.; Reutt-Robey, J. E. Coverage Dependent Supramolecular Structures: C₆₀:ACA Monolayers on Ag(111). *J. Am. Chem. Soc.* **2006**, *128*, 8493–8499.
28. Bonifazi, D.; Kiebele, A.; Stöhr, M.; Cheng, F.; Jung, T.; Diederich, F.; Spillmann, H. Supramolecular Nanostructuring of Silver Surfaces via Self-Assembly of [60]Fullerene and Porphyrin Modules. *Adv. Funct. Mater.* **2007**, *17*, 1051–1062.
29. Wakayama, Y.; de Oteyza, D. G.; Garcia-Lastra, J. M.; Mowbray, D. J. Solid-State Reactions in Binary Molecular Assemblies of F₁₆CuPc and Pentacene. *ACS Nano* **2011**, *5*, 581–589.
30. Nakaya, M.; Kuwahara, Y.; Aono, M.; Nakayama, T. Reversibility-Controlled Single Molecular Level Chemical Reaction in a C₆₀ Monolayer via Ionization Induced by Scanning Tunneling Microscope. *Small* **2008**, *4*, 538–541.
31. Akai-Kasaya, M.; Shimizu, K.; Watanabe, Y.; Saito, A.; Aono, M.; Kuwahara, Y. Electronic Structure of a Polydiacetylene Nanowire Fabricated on Highly Ordered Pyrolytic Graphite. *Phys. Rev. Lett.* **2003**, *91*, 255501.
32. Nakaya, M.; Tsukamoto, S.; Kuwahara, Y.; Aono, M.; Nakayama, T. Molecular Scale Control of Unbound and Bound C₆₀ for Topochemical Ultradense Data Storage in an Ultrathin C₆₀ Film. *Adv. Mater.* **2010**, *22*, 1622–1625.
33. Neumann, W.; Sixl, H. The Mechanism of the Low Temperature Polymerization Reaction in Diacetylene Crystals. *Chem. Phys.* **1981**, *58*, 303–312.
34. Win, W. W.; Kao, M.; Eiermann, M.; McNamara, J. J.; Wudl, F. Methyl 1,2-Dihydrofullerenecarboxylate. *J. Org. Chem.* **1994**, *59*, 5871–5876.
35. Osterodt, J.; Vögtle, F. C₆₁Br₂: A New Synthesis of Dibromomethanofullerene and Mass Spectrometric Evidence of the Carbon Allotropes C₁₂₁ and C₁₂₂. *Chem. Commun.* **1996**, 547–548.
36. Fabre, T. S.; Treleaven, W. D.; McCarley, T. D.; Newton, C. L.; Landry, R. M.; Saraiva, M. C.; Strongin, R. M. The Reaction of Buckminsterfullerene with Diazotetrazole. Synthesis, Isolation, and Characterization of (C₆₀)₂C₂. *J. Org. Chem.* **1998**, *63*, 3522–3523.
37. Fernández, G.; Pérez, E. M.; Sánchez, L.; Martín, N. Self-Organization of Electroactive Materials: A Head-to-Tail Donor–Acceptor Supramolecular Polymer. *Angew. Chem., Int. Ed.* **2008**, *47*, 1094–1097.
38. Sakamoto, K.; Harada, M.; Kondo, D.; Kimura, A.; Kakizaki, A.; Suto, S. Bonding State of the C₆₀ Molecule Adsorbed on a Si(111)-(7 × 7) Surface. *Phys. Rev. B* **1998**, *58*, 13951.
39. Lu, X.; Grobis, M.; Khoo, K. H.; Louie, S. G.; Crommie, M. F. Charge Transfer and Screening in Individual C₆₀ Molecules on Metal Substrates: A Scanning Tunneling Spectroscopy and Theoretical Study. *Phys. Rev. B* **2004**, *70*, 115418.
40. Wang, H.; He, Y.; Li, Y.; Su, H. Photophysical and Electronic Properties of Five PCBM-like C₆₀ Derivatives: Spectral and Quantum Chemical View. *J. Phys. Chem. A* **2012**, *116*, 255–262.
41. Stojkovic, S.; Joachim, C.; Grill, L.; Moresco, F. The Contact Conductance on a Molecular Wire. *Chem. Phys. Lett.* **2005**, *408*, 134–138.
42. Moresco, F.; Gross, L.; Alemani, M.; Rieder, K.-H.; Tang, H.; Gourdon, A.; Joachim, C. Probing the Different Stages in Contacting a Single Molecular Wire. *Phys. Rev. Lett.* **2003**, *91*, 036601.
43. Nakaya, M.; Aono, M.; Nakayama, T. Molecular-Scale Size Tuning of Covalently Bound Assembly of C₆₀ Molecules. *ACS Nano* **2011**, *5*, 7830–7837.